Supplementary Material

Effect of horizontal divergence on estimates of firn-air content

Annika N. HORLINGS,[1] Knut CHRISTIANSON,[1] Nicholas HOLSCHUH,[2] C. Max STEVENS,[1] Edwin D. WADDINGTON[1]

[1] Department of Earth and Space Sciences, University of Washington, Seattle, WA, USA

[2]Department of Geology, Amherst College, Amherst, MA 01002

annikah2@uw.edu

1 The Community Firn Model and the layer-thinning scheme in detail

The Community Firn Model (CFM; Stevens and others, 2020) simulates the evolution of firn properties in a modular one-dimensional Lagrangian framework. Users specify the surface-boundary conditions (accumulation rate, temperature, and/or surface-snow density), firn-densification physics, time step, and thickness of the model domain to use. The CFM runs by first spinning up the specified model to steady state to create an initial condition for the primary model run. The spin-up must have sufficient duration to evolve the firn-column properties to reset the entire domain. The Lagrangian domain consists of a fixed number of parcels representing layers of firn. Parcels are added at the ice-sheet surface and removed at depth once the parcels reach ice density. After spinning up, the CFM evolves the firn column in response to the varying boundary conditions.

The Lagrangian vertical strain rate $\dot{\varepsilon}_{zz}$ in the firn is generally related to the Lagrangian densification rate through:

$$\dot{\varepsilon}_{zz} = -\frac{1}{\rho}\frac{D\rho}{Dt} \tag{S1}$$

where ρ is the firn density, t is time, and z is the depth. Most firn-compaction models employ a form of the compaction equation that solves for the Lagrangian rate of change of density $\frac{D\rho}{Dt}$:

$$\frac{D\rho}{Dt} = c(\rho_i - \rho) \tag{S2}$$

where t is time and c is a coefficient that is usually calibrated to fit the model results to depth-density profiles, which are assumed to be in steady-state. These coefficients are broadly speaking representative of physical firn-densification mechanisms (Lundin and others, 2017; Stevens and others, 2020). In a steady-state firn column, the model form of Equation S2 is compatible with the suggestion by Robin (1958) that the fractional change in porosity with depth, and therefore change of density with depth, is proportional to the increment of additional overburden load. This was originally expressed as:

$$\frac{D\rho}{Dz} = \beta g \rho(\rho_i - \rho) \tag{S3}$$

where β is a constant and g is gravity. The CFM solves density evolution $\frac{d\rho}{dt}$ explicitly (Equation 2 in Stevens and others (2020)) through:

$$\rho_{new} = \rho_{old} + \left(\frac{d\rho}{dt}\right) dt. \quad \text{(S4)}$$

We next show how firn-parcel thickness λ relates to firn density ρ. We can express changes in λ due to the vertical strain rate (i.e., due to a traditional firn-compaction model) as:

$$\lambda_{part1} = \lambda_{old}(1 + \dot{\varepsilon}_{zz}\Delta t). \quad \text{(S4)}$$

Alternatively, this can be expressed in terms of density changes and the derivative $\frac{D\rho}{Dt}$ that most firn-compaction models solve for:

$$\lambda_{part1} = \lambda_{old}\left(1 - \left(\frac{1}{\rho}\frac{D\rho}{Dt}\right)\Delta t\right) \quad \text{(S5)}$$

which can then be expressed using Equation S2:

$$\lambda_{part1} = \lambda_{old} - \lambda_{old} c\Delta t(\rho_i - \rho). \quad \text{(S6)}$$

In the layer-thinning scheme, the firn parcels are further thinned due to stretching from a prescribed rate of horizontal divergence $\dot{\varepsilon}_h$:

$$\lambda_{part2} = \lambda_{part1}(1 + \dot{\varepsilon}_h\Delta t). \quad \text{(S7)}$$

The resulting thinned parcel thickness λ_{total} of the firn parcels during a single time step using the layer-thinning scheme can be expressed as:

$$\lambda_{total} = \lambda_{old} - \lambda_{old} c\Delta t(\rho_i - \rho)(1 + \dot{\varepsilon}_h\Delta t) = \lambda_{old} - (\lambda_{old} c(\rho_i - \rho) + \lambda_{old} c\dot{\varepsilon}_h\Delta t)\Delta t \quad \text{(S8)}$$

where the selected firn-compaction model (e.g., Herron and Langway (1980); Ligtenberg and others, 2011) solves for the vertical strain rate given by the general form $c\left(\frac{\rho_i - \rho}{\rho}\right)$, and the rate of horizontal divergence $\dot{\varepsilon}_h$is a specified condition in the CFM. Equation S8 implements a continuity assumption, i.e., $\dot{\varepsilon}_h = \dot{\varepsilon}_{zz}$.

2 Notes on Morris and others (2017) approach to thinning

Morris and others (2017) consider horizontal divergence in their estimation of the density-corrected vertical strain rate F_Z, by subtracting a correction to the density-corrected volumetric strain rate without horizontal divergence $F(\rho)$ in terms of the mean density ρ_m over time Δt, ice density ρ_i, and horizontal divergence $\dot{\varepsilon}_h$ (Equation 19 of Morris and others (2017)):

$$F_Z(\rho) \approx F(\rho) - \left(\frac{\rho_m}{\rho_i - \rho_m}\right)\dot{\varepsilon}_h \quad \text{(S9)}$$

where horizontal divergence is estimated from neutron probe firn data determined through (Equation 18 of Morris and others (2017)):

$$q_i(i) \approx (1 + \dot{\varepsilon}_H\Delta t)q_2(i) \quad \text{(S10)}$$

where $q_i(i)$ is the initial water-equivalent height in the firn column, which moves to water-equivalent height $q_2(i)$ after time step Δt. Equation S10 is equivalent to Equation S7, where q represents water-equivalent height instead of thickness λ of the firn parcel.

3 Differences between the Herron and Langway (1980) and Ligtenberg and others (2011) firn-compaction models

The Herron and Langway (1980) firn-compaction model (HL) assumes that firn compaction is dependent on two commonly measured variables: mean annual accumulation rate, and mean annual surface temperature. HL used Sorge's Law (Bader, 1954) and depth-density profiles from seven sites in Greenland and ten sites in Antarctica to derive their model. Sorge's Law is the steady-state relation:

$$v(z) = \frac{\dot{b}}{\rho(z)} \tag{S11}$$

where $v(z)$ is the vertical velocity of a parcel of firn and $\dot{b}$ is the accumulation rate. Equation S11 can be differentiated with respect to depth to allow the vertical strain rate to be estimated from a depth-density profile:

$$\dot{\varepsilon}_{zz} = \frac{\partial v}{\partial z} \approx \frac{\partial \rho}{\partial z}\frac{\dot{b}}{\rho^2} \tag{S12}$$

HL empirical solution for stages 1 and 2 of the firn column, respectively, is:

$$\frac{D\rho}{Dt} = k_0 A^a(\rho_i - \rho), \quad \rho < 550\ kg\ m^{-3} \tag{S13}$$

$$\frac{D\rho}{Dt} = k_1 A^b(\rho_i - \rho), \quad 550\ kg\ m^{-3} < \rho < 800\ kg\ m^{-3} \tag{S14}$$

where *A* is the accumulation rate; the accumulation constants $a = 1.1 \pm 0.2$ and $b = 0.5 \pm 0.2$; and the Arrhenius-type rate constants are:

$$k_0 = 11exp\left[-\frac{10160}{RT}\right] \tag{S15}$$

$$k_1 = 575exp\left[-\frac{21400}{RT}\right]. \tag{S16}$$

The Ligtenberg and others (2011) firn-compaction model (LIG) is based on the steady-state version of the Arthern and others (2010) model (ART-S). ART-S is based on the form of HL, but uses vertical strain rate data from three sites in Antarctica, instead of depth-density data and Sorge's Law, to derive its coefficients. LIG added a tuning coefficient to adjust the accumulation dependence in ART-S to expand applicability to more sites on the ice sheets. LIG solves the equations:

$$\frac{D\rho}{Dt} = M_0 C_0 F\dot{b}g(\rho_i - \rho), \quad \rho < 550\ kg\ m^{-3} \tag{S17}$$

$$\frac{D\rho}{Dt} = M_1 C_1 F\dot{b}g(\rho_i - \rho), \quad 550\ kg\ m^{-3} < \rho < 800\ kg\ m^{-3} \tag{S18}$$

where g is gravitation acceleration, $\dot{b}$ is the average annual accumulation rate, $M_0 = 1.435 - 0.151ln(\dot{b})$ and $M_1 = 2.366 - 0.293ln(\dot{b})$; the constants are $C_0 = 0.03$ and $C_1 = 0.07$; and the Arrhenius-type rate constants are:

$$F = exp\left[-\frac{E_C}{RT} + \frac{E_g}{RT}\right] \quad \text{(S19)}$$

where R is the ideal gas constant, T is temperature, $E_C = 60\ kJ\ mol^{-1}$, and $E_g = 42.4\ kJ\ mol^{-1}$.

4 Estimates of firn-air content in mass-change estimates

FAC changes in time (ΔFAC) are important for altimetry studies of ice-sheet mass balance in order to determine changes in mass Δm from observed changes ice-sheet surface elevation Δh_{obs}. Model estimates of ΔFAC can be subtracted from the time series of total surface-elevation change h to produce a time series of ice-equivalent thickness change (Shepherd and others, 2012; Depoorter and others, 2013; Shepherd and others, 2019). The mass of the ice column can be described in terms of observed column volume (thickness h_{obs}, area A, FAC, and density ρ_i):

$$m = h_{obs} - (FAC)\rho_i A. \quad \text{(S20)}$$

We are interested in Δm, which is defined as the difference between the mass evaluated at the current time m^k and the mass evaluated at a previous time m^{k-1}:

$$\Delta m = m^k - m^{k-1}. \quad \text{(S21)}$$

Similarly, ΔFAC is the difference between the FAC evaluated at a more current time $FAC^{\,k}$ and the FAC evaluated at a previous time FAC^{k-1}. Then, the change in mass can be expressed in terms of the ΔFAC:

$$m^k - m^{k-1} = \left(h_{obs}^k - (FAC^k)\right)\rho_i A - \left(h_{obs}^{k-1} - (FAC^{k-1})\right)\rho_i A \quad \text{(S22)}$$

$$\Delta m = (\Delta h - \Delta FAC)\rho_i A. \quad \text{(S23)}$$

As we determine the impact of horizontal divergence on FAC, Equation S23 allows us to assess its impact on the calculated change in mass from a change in elevation.

5 Herron and Langway (1980) results

Figures 5-7 in the main text show the results of LIG. Below, we show the results from the same runs using HL.

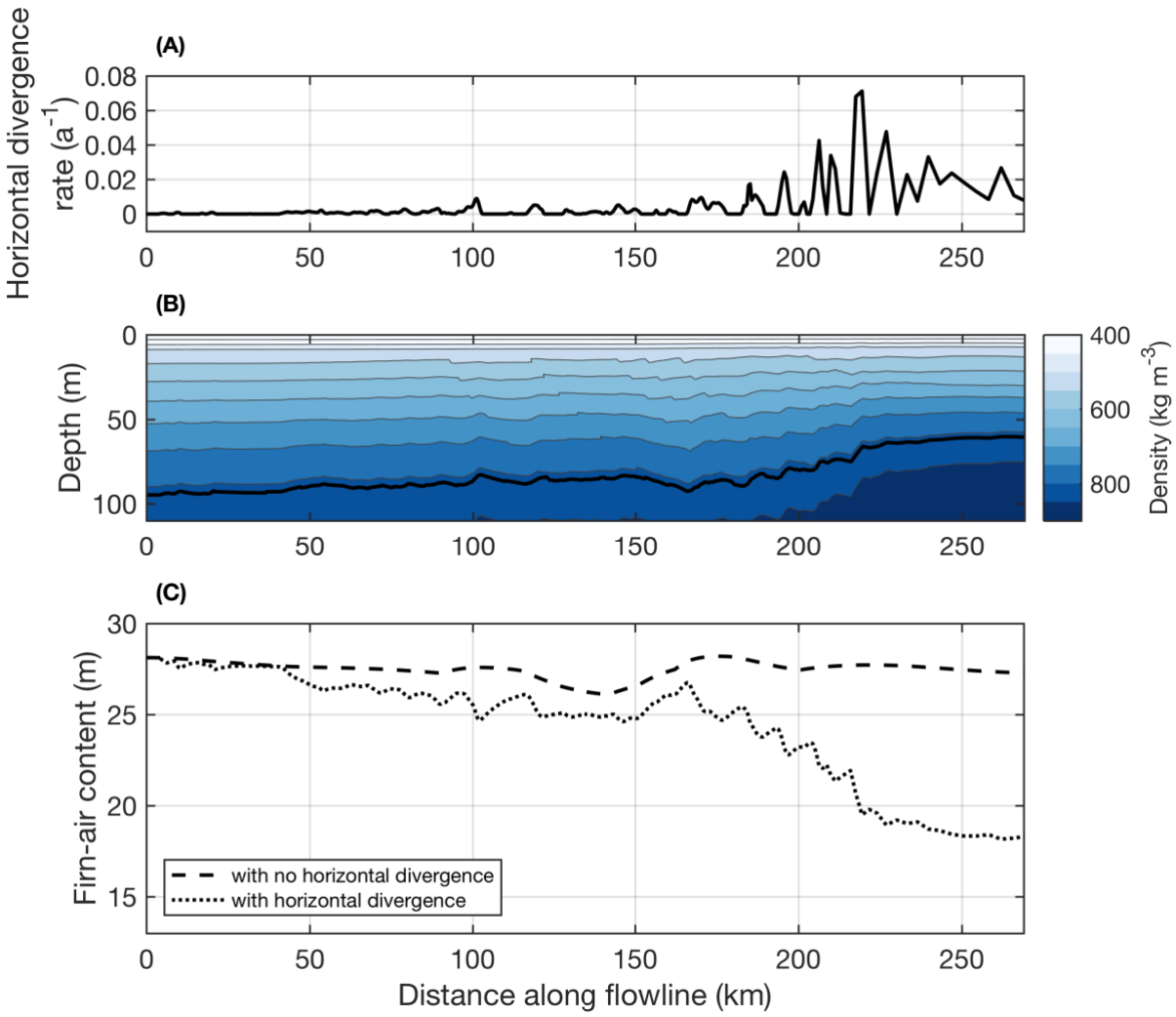

Figure S1. Results from the layer-thinning scheme for the flowline on Thwaites Glacier using the Herron and Langway (1980) firn-compaction model (Experiment 2). (A) Horizontal divergence rates for the flowline. Horizontal divergence rates were derived from Mouginot and others (2019) following the approach of Alley and others (2018), and exclude compression. (B) The firn depth-density profiles along the flowline for the model that accounts for horizontal divergence. Black line indicates bubble close-off (BCO) depth (i.e., density of 830 kg m^{-3}). Contour interval is 50 kg m^{-3}. (C) FAC results from model runs including the horizontal divergence rates shown in (A) (dotted line) and from a model without the horizontal divergence rates (dashed line).

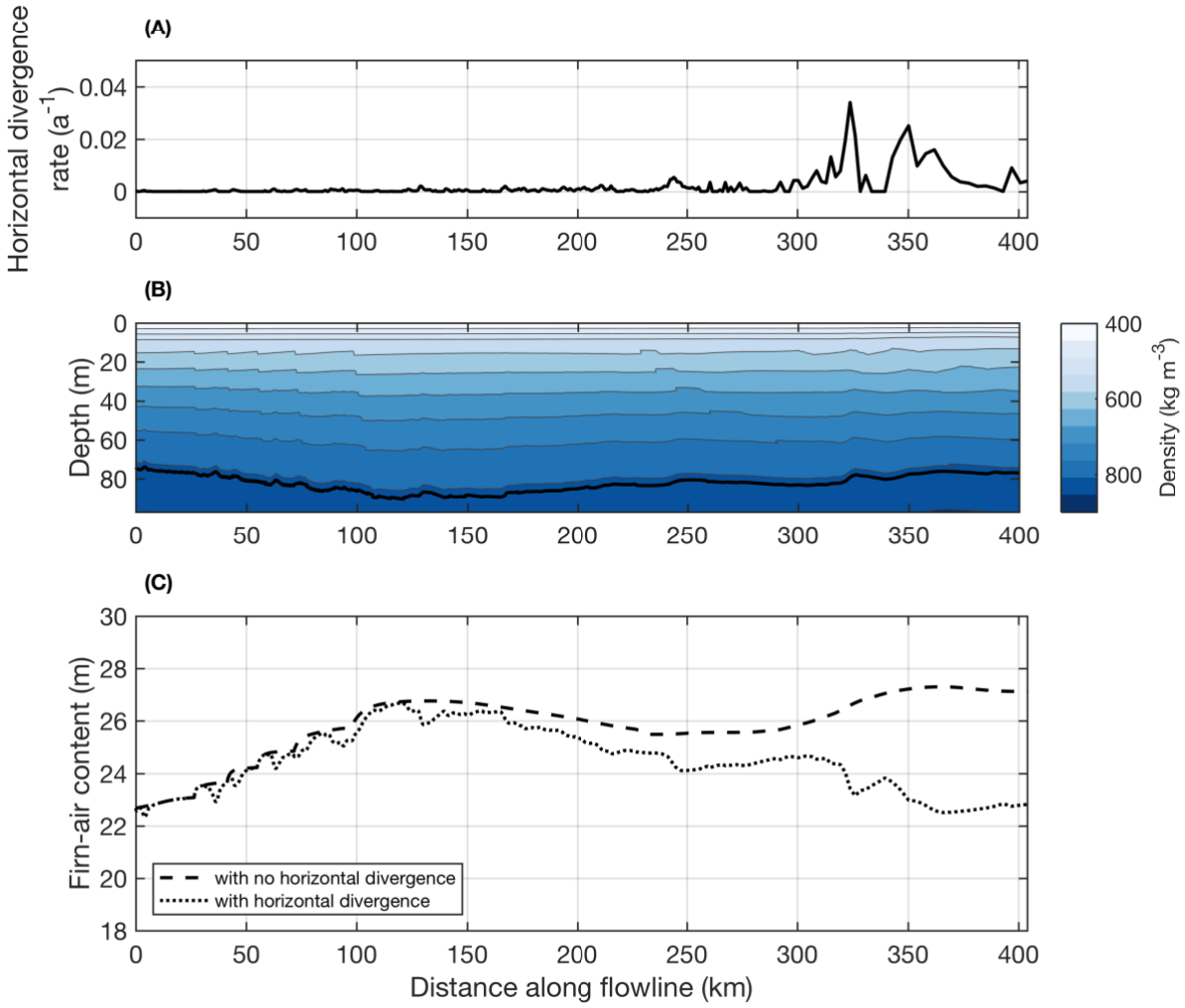

Figure S2. Results from the layer-thinning scheme for a flowline on Pine Island Glacier using the Herron and Langway (1980) firn-compaction model (Experiment 3). (A) Horizontal divergence rates for the flowline. Horizontal divergence rates were derived from Mouginot and others (2019) following the approach of Alley and others (2018), and exclude compression. (B) The firn depth-density profiles along the flowline for the model that accounts for horizontal divergence. Black line indicates bubble close-off (BCO) depth (i.e., density of 830 kg m^{-3}). Contour interval is 50 kg m^{-3}. (C) FAC results from model runs with the horizontal divergence rates shown in (A) (dotted line) and from a model without horizontal divergence rates (dashed line).

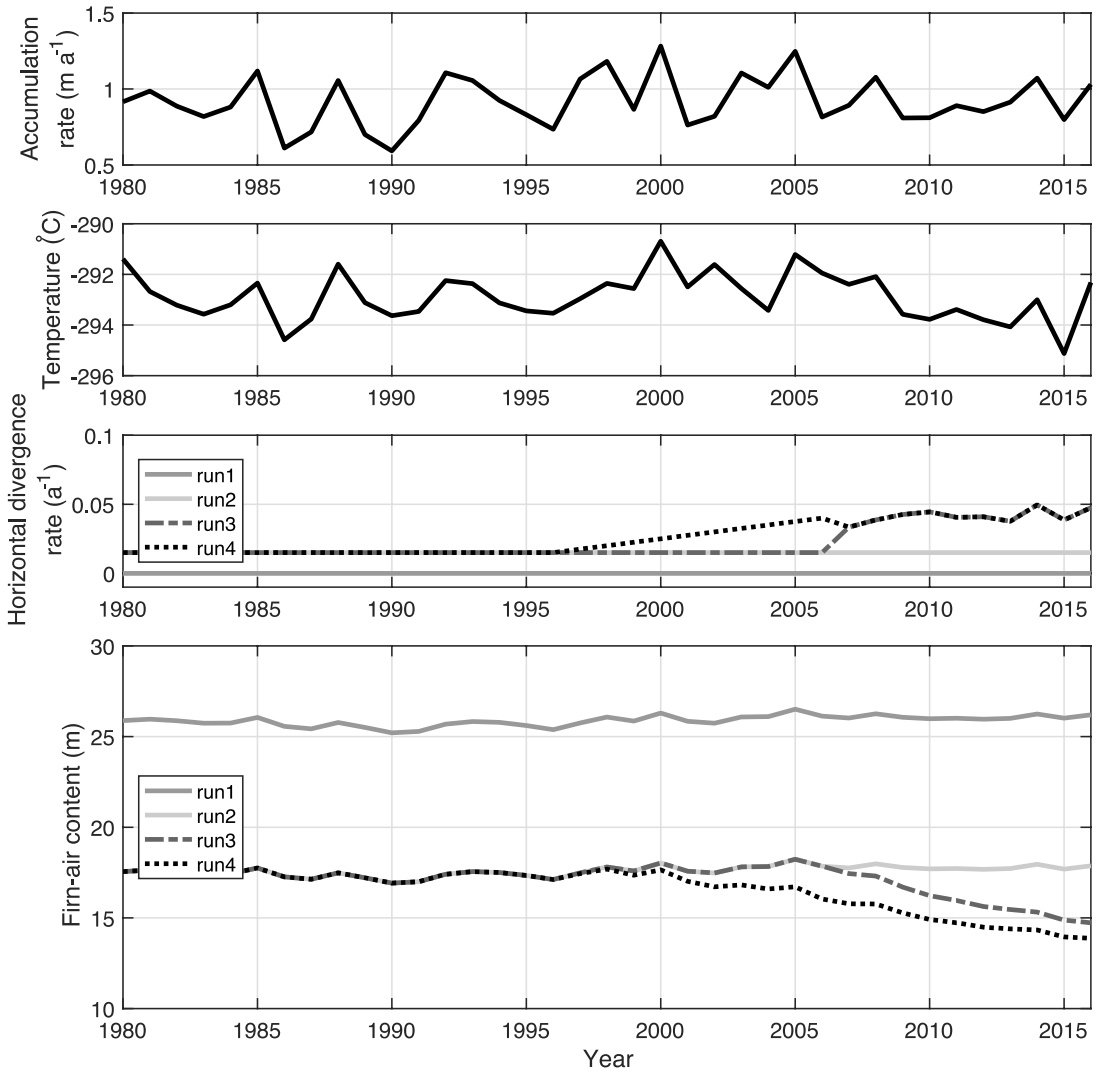

Figure S3. Surface boundary conditions, horizontal divergence rates, and estimated FAC using the layer-thinning scheme with the Herron and Langway (1980) firn-compaction model for a location on lower Thwaites Glacier (Experiment 4). A portion of the model spin up is shown from 1980 to 2007. Run 1 represents a conventional firn-compaction model run with no horizontal divergence. A constant horizontal divergence rate of 0.015 a^{-1} is used in run 2. For runs 3 and 4, after spin up with a constant divergence rate of 0.015 a^{-1}, the model is run from 2007 to 2016 with temporally variable horizontal divergence rates derived from the Mouginot and others (2017) velocity time series. Run 4 includes a linear ramp between horizontal divergence rates from the 1997 to 2007 values.

References

Alley KE, Scambos TA, Anderson RS, Rajaram H, Pope A, and Haran TM (2018) Continent-wide estimates of Antarctic strain rates from Landsat 8-derived velocity grids. *Journal of Glaciology*, 64 (244), 321-32 (doi: 10.1017/jog.2018.23)

Arthern RJ, Vaughan DG, Rankin AM, Mulvaney R and Thomas ER (2010) In situ measurements of Antarctic snow compaction compared with predictions of models. *Journal of Geophysical Research: Earth Surface*, 115(F03011) (doi: 10.1029/2009JF001306)

Bader, H (1954) Sorge's Law of densification of snow on high polar glaciers. *Journal of Glaciology*, 2(15), 319-323 (doi: 10.3189/S0022143000025144)

Herron MM and Langway CC (1980) Firn densification: an empirical model. *Journal of Glaciology*, 25(93), 373–385 (doi: 10.3189/S0022143000015239)

Ligtenberg S, Helsen M and Van den Broeke M (2011) An improved semi-empirical model for the densification of Antarctic firn. *The Cryosphere*, 5, 809–819 (doi: 10.5194/tc-5-809-2011)

Robin, GDQ (1958) Seismic shooting and related investigations, Glaciology III. *Norwegian-British-Swedish Antarctic Expedition, 1949–52, Scientific results*, V 7-135

Stevens CM, Verjans V, Lundin J, Kahle, EC, Horlings AN, Horlings BI and Waddington, ED (2020). The Community Firn Model (CFM) v1. 0. *Geoscientific Model Development Discussions*, 1-37 (doi: 10.5194/gmd-2019-361)